AD-A134 759 VARIATION OF LASER ABSORPTION WITH PLASMA SCALELENGTH IN LONG-SCALELENGTH PLASMAS(U) NAVAL RESEARCH LAB WASHINGTON DC M J HERBST ET AL. 30 SEP 83 NRL-MR-5186 1/1

UNCLASSIFIED F/G 20/9 NL

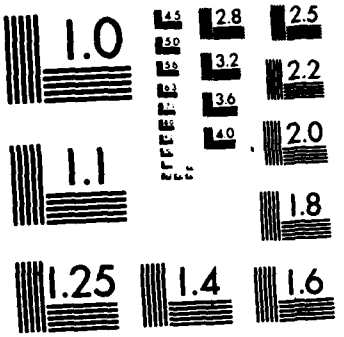

(2)

NRL Memorandum Report 5186

AD-A134 759

Variation of Laser Absorption with Plasma Scalelength in Long-Scalelength Plasmas

M. J. HERBST, J. GRUN,* J. GARDNER,** J. A. STAMPER, F. C. YOUNG,†
S. P. OBENSCHAIN, E. A. MCLEAN, AND B. H. RIPIN

Laser Plasma Branch
Plasma Physics Division

**Mission Research Corporation*
Alexandria, VA 22312

***Laboratory for Computational Physics*

†Plasma Technology Branch
Plasma Physics Division

September 30, 1983

This work was sponsored by the U.S. Department of Energy.

NAVAL RESEARCH LABORATORY
Washington, D.C.

SECURITY CLASSIFICATION OF THIS PAGE (When Data Entered)

REPORT DOCUMENTATION PAGE		READ INSTRUCTIONS BEFORE COMPLETING FORM
1. REPORT NUMBER NRL Memorandum Report 5186	2. GOVT ACCESSION NO. AD-A134759	3. RECIPIENT'S CATALOG NUMBER
4. TITLE (and Subtitle) VARIATION OF LASER ABSORPTION WITH PLASMA SCALELENGTH IN LONG-SCALELENGTH PLASMAS		5. TYPE OF REPORT & PERIOD COVERED Interim report on a continuing NRL problem. 6. PERFORMING ORG. REPORT NUMBER
7. AUTHOR(s) M.J. Herbst, J. Grun,* J. Gardner, J.A. Stamper, F.C. Young, S.P. Obenschain, E.A. McLean, and B.H. Ripin		8. CONTRACT OR GRANT NUMBER(s)
9. PERFORMING ORGANIZATION NAME AND ADDRESS Naval Research Laboratory Washington, DC 20375		10. PROGRAM ELEMENT, PROJECT, TASK AREA & WORK UNIT NUMBERS DOE AI-08-79DP40092(172); 47-0859-0-3
11. CONTROLLING OFFICE NAME AND ADDRESS U.S. Department of Energy Washington, DC 20545		12. REPORT DATE September 30, 1983 13. NUMBER OF PAGES 11
14. MONITORING AGENCY NAME & ADDRESS(if different from Controlling Office)		15. SECURITY CLASS. (of this report) UNCLASSIFIED 15a. DECLASSIFICATION/DOWNGRADING SCHEDULE

16. DISTRIBUTION STATEMENT (of this Report)

Approved for public release; distribution unlimited.

17. DISTRIBUTION STATEMENT (of the abstract entered in Block 20, if different from Report)

18. SUPPLEMENTARY NOTES

*Present address: Mission Research Corporation, Alexandria, VA 22312

This work was sponsored by the U.S. Department of Energy.

19. KEY WORDS (Continue on reverse side if necessary and identify by block number)

Laser-plasma interactions
Stimulated Brillouin backscatter
Plasma production and heating by lasers
Plasma instabilities
Electromagnetic wave propagation in plasma

20. ABSTRACT (Continue on reverse side if necessary and identify by block number)

A short-pulse, high-intensity Nd-laser beam interacts with preformed plasmas of variable scalelength. At the longest scalelength, absorption is limited by backscatter, despite increased collisional absorption.

DD FORM 1 JAN 73 1473 EDITION OF 1 NOV 65 IS OBSOLETE
S/N 0102-014-6601

SECURITY CLASSIFICATION OF THIS PAGE (When Data Entered)

CONTENTS

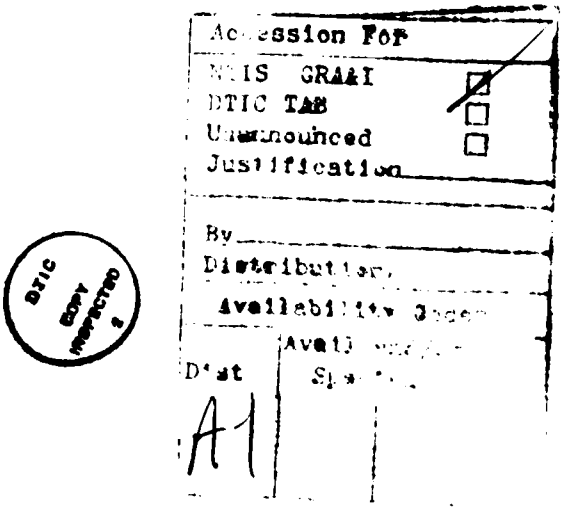

VARIATION OF LASER ABSORPTION WITH PLASMA SCALELENGTH IN LONG-SCALELENGTH PLASMAS

The achievement of high-gain laser fusion depends upon the efficient absorption of laser light in the underdense plasma surrounding the fuel pellet. In addition to the absorption efficiency, the absorption mechanisms are important: a premium is placed upon collisional absorption, which preferentially produces thermal particle distributions. Other absorption processes tend to produce energetic particles, which may penetrate the fuel-pellet shell and preheat the fuel, thereby impeding the compression required for high gain.

The blend of absorption processes which dominates in small plasmas is likely to be entirely different from that which dominates in large plasmas, because the effectiveness of each of the processes varies differently with the density inhomogeneity scalelength $L_n \equiv |n/\nabla n|$. For example, the resonance absorption process,[1] shown to dominate in small plasmas,[2] becomes less important with longer L_n, while collisional absorption[3] becomes more important. Unfortunately, parametric instabilities[4] also become more effective in larger plasmas; these can either degrade absorption efficiency by scattering incident laser light or degrade absorption quality by generating energetic particles. Experimental studies of this changing role of different absorption processes are important because large, high-gain pellets will be surrounded by much larger plasmas than in recent experiments. In this work, we describe the first long-scalelength experiments with controlled variations of plasma scalelength. As the scalelength increases, backscatter limits the absorption efficiency despite an increased effectiveness of collisional absorption.

To study high-intensity laser absorption in long-scalelength plasmas, we use a novel configuration of our two-beam, Nd (λ_o = 1.054 μm) laser. One beam generates long-scalelength background plasmas; it has a 4-nsec duration and irradiates a large area (90% of the energy within a diameter $d_{90} \approx 1080$ μm), giving a peak irradiance of about 6×10^{12} W/cm^2 at the surface of the polystyrene foil target. To produce higher irradiances for absorption studies, we tightly focus our second beam (50% of the energy within $d_{50} \approx 90$ μm) along the central axes of the plasmas produced by the first beam. The second beam is synchronous with the peak of the first beam, and its pulse duration is reduced to 300 psec to minimize hydrodynamic perturbations to the background plasmas. Vacuum intensities (averaged within d_{50}) in the short pulse vary between 10^{14} and 10^{15} W/cm^2 for incident energies E between 4 and 40 J. Actual intensities in the plasma may be altered by self-focusing; for that reason, incident energies are quoted in the text. Initially, the two beams have orthogonal linear polarizations, but passage through a quarter-wave plate produces opposite circular polarizations at the target, and converts circularly polarized backscatter to linear polarization before detection.

Plasma characterization. The background scalelength is varied by aperturing the background beam so as to reduce d_{90} from 1080 μm to either 640 μm or 360 μm; hereafter, we refer to these as the long, medium, and short-scalelength background plasmas, respectively. Density profiles measured by third-harmonic interferometry are shown in Fig. 1 and compared with predictions of our hydrodynamics code,[5] a 2-D, cylindrical model with collisional

Manuscript approved August 22, 1983.

absorption and classical thermal conduction. Although axial shifts have been made in this comparison due to uncertainty in the target position, the data confirms code-predicted scalelengths at given densities. At 0.1 critical density, for example, L_n/λ_o varies from 200 to 400 as the spot size is increased. The overdense plasma seems unaffected by the lateral expansion at these spot sizes: L_n/λ_o at critical density is predicted by the code to be near 45 for all three background conditions. Plasma velocity profiles, important for Brillouin scattering,[4] are not shown but are directly related to the density profiles by the hydrodynamics. The background plasmas have nearly the same peak temperature, because the beam is apertured so as to maintain nearly the same irradiance; the code predicts a variation from 460 eV in the short-scalelength plasma to 525 eV in the long-scalelength plasma.

Additional plasma heating results from irradiation by the high-intensity beam. This is monitored by measuring thermal x-ray emission with two subnanosecond scintillator-photodiodes filtered to look at 1.0-1.5 and 2.0-2.8 keV x rays, respectively.[6] Ratios of these detector signals imply time-averaged temperatures during the short pulse which are factors of 1.1 to 1.8 higher than the peak background temperatures for short-pulse energies of 4 J to 40 J. These temperature increases are consistent with estimates from free-bound continuum spectra predicted by the 2-D code, although calculated temperatures are 10-15% higher than measured temperatures.

This localized heating can cause density perturbations. The creation of density channels along the laser axis in the underdense plasma is experimentally inferred from time-integrated images of second-harmonic emission obtained for $E \gtrsim 15$ J.[7] This data also provides evidence for self-focusing of the beam in these channels. For $E < 15$ J, the images infrequently indicate density channels and almost never suggest self-focusing.

The 2-D code also predicts density perturbations which strengthen with increasing incident energy. As E increases from 5J to 25J, on-axis density minima form earlier in time and over greater radial extent. The maximum depth $\Delta n/n$ increases from about 5% at 5J to about 15% at 25J. These may be lower bounds on $\Delta n/n$, however, since the code does not include beam refraction by these perturbations (i.e., self-focusing). The code also predicts axial perturbations; a shock propagates down the density gradient into the underdense plasma, perhaps as a transient response to the increased mass-ablation rate of the higher intensity beam. With increased incident energy, this shock strengthens and occurs at earlier times.

Scattered Light and Absorption. Backscatter through the incident f/6.7 lens is observed with both time-resolving and time-integrating detectors. A photodiode with 700 psec risetime distinguishes short-pulse backscatter from the lower level of long-pulse backscatter. Quoted reflectivities are energy reflectivities of the short pulse, since this detector cannot resolve within the short pulse. Backscattered energy is monitored using two calorimeters, one for each polarization. The short-pulse backscatter is preferentially polarized with the polarization of the high-intensity beam, unlike the unpolarized backscatter of the background beam. Backscatter reflectivities, as shown in Fig. 2, increase with incident energy for $E \lesssim 15$J, but decrease at higher energies.

Properties of the backscatter are consistent with production by stimulated Brillouin scattering.[4] Backscattered light has the polarization of the incident beam. For $E \lesssim 15$ J, the reflectivity R increases with incident energy and the rate of this increase becomes greater with increased scalelength. While R decreases for E > 15J, this may be due to the strong plasma perturbations at higher incident energies. The axial shock predicted by the code, for example, could reduce Brillouin backscatter since it produces an abrupt change in the plasma velocity profile. This apparent backscatter reduction could also be due to an increased angular spread of backscatter at higher incident energies, since scattered light just outside the incident lens cone is not monitored.

Light scattered outside of the incident focal cone is measured with five subnanosecond diodes: four detectors are deployed on one side of the specular angle (12°) in the plane of incidence of the laser, and the fifth samples light on the other side. If we assume symmetry about the specular direction, as shown in Fig. 3A, we can infer the total amount of scattered light outside the incident lens cone. In contrast to direct backscatter, the amount of this light decreases with increasing background scalelength. The reflectivity S integrated over the angular distribution varies with incident energy as shown in Figs. 3B-D.

The observations of scattered light outside the lens cone are consistent with the hypothesis that this is non-absorbed light that has been specularly reflected from the critical-density surface. The decrease of S at longer scalelength can be explained by increased collisional absorption, which reduces the penetration of ingoing light to critical density and of outgoing reflected light to the detectors. The increase of S with incident energy can be explained by increased plasma heating, which reduces collisional absorption.

Experimental absorption fractions $\eta = 1-R-S$ are close to code predictions for collisional absorption alone. (For this comparison, the incident energy in the code is reduced by the observed backscatter.) As shown in Fig. 4, experimental values of η are consistent with or slightly greater than calcuated values, but by no more than 10% of the incident energy. This slight gap has at least three possible explanations: 1) with the limited number of detectors, some scattered laser light may be missed, causing an overestimate of the experimental absorption, 2) the code may underestimate the collisional absorption since it gives slightly higher x-ray temperatures than are measured, and 3) absorption mechanisms other than collisional absorption may be operative. None of these alternatives significantly affects the inferred absorption fractions, although explanation (3) raises concern about generation of suprathermal particles by the additional absorption mechanism(s).[6]

Although the absorption fractions seem mainly due to a combination of collisional absorption and backscatter, the mechanism that limits η changes with the background scalelength. We restrict ourselves to $E \lesssim 15$ J, where effects of plasma perturbations are believed to be minimal. For the short scalelength, we find low levels of backscatter and at least an equal amount of scattered light at other angles. If the latter is specular scatter, we infer that η is limited primarily by the inefficiency of collisional absorption in the short-scalelength plasma; even without backscatter, collisional absorption could not greatly increase. In contrast, the long-scalelength case exhibits larger backscatter and little scattered light at other angles; we infer that

collisional absorption is very efficient, and that backscatter now limits the absorption fraction.

These observations have important implications for laser fusion. Plasmas surrounding high-gain pellets will differ significantly from those of the present experiment: scalelengths are expected to be longer by factors of five or more and temperatures are predicted to be greater by factors of two or more. Collisional absorption is expected to be at least as efficient in these plasmas as in the present experiment because the effect of longer scalelength tends to offset that of increased temperature. Levels of backscatter, on the other hand, will depend upon ion-wave damping rates and instability noise levels,[4] which may differ from those of the present experiment. Nonetheless, with the much longer scalelengths, backscatter may severely reduce absorption efficiencies in these plasmas. Hopefully, proposed mechanisms,[8] such as shorter laser wavelength or wider laser bandwidth, will be sufficient to control backscatter.

Although the new experimental approach described here allows study of longer scalelengths with a given laser energy and enables one to vary the scalelength in a controlled manner, it has limitations. First, one must allow for possible effects on the results due to the perturbations of the background plasma. Second, the limited diameter of the high-intensity beam may prevent adequate simulation of some plasma instabilities (e.g., Brillouin sidescatter) that require a larger transverse interaction region.

The authors wish to acknowledge valuable conversations with Dr. S.E. Bodner and Dr. R.H. Lehmberg. We also appreciate the technical assistance of M. Fink, K. Kearney, J. Kosakowski, N. Nocerino, E. Turbyfill and B. Sands. This work was supported by the U.S. Department of Energy and the Office of Naval Research.

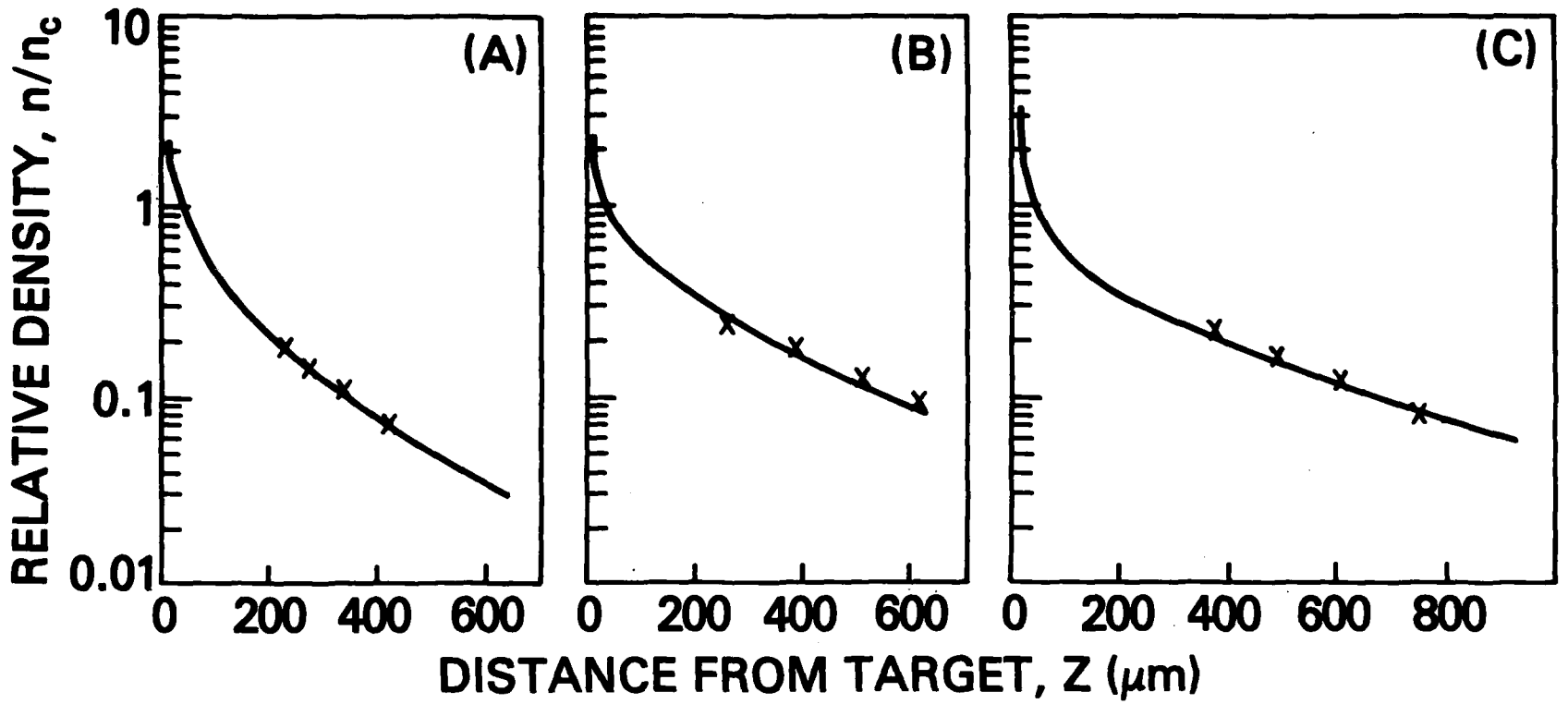

Fig. 1. On-axis profiles of density n relative to critical density n_c. 2-D code results (solid curve) and interferometric results (points) for: (A) short, (B) medium, and (C) long-scalelength background plasmas.

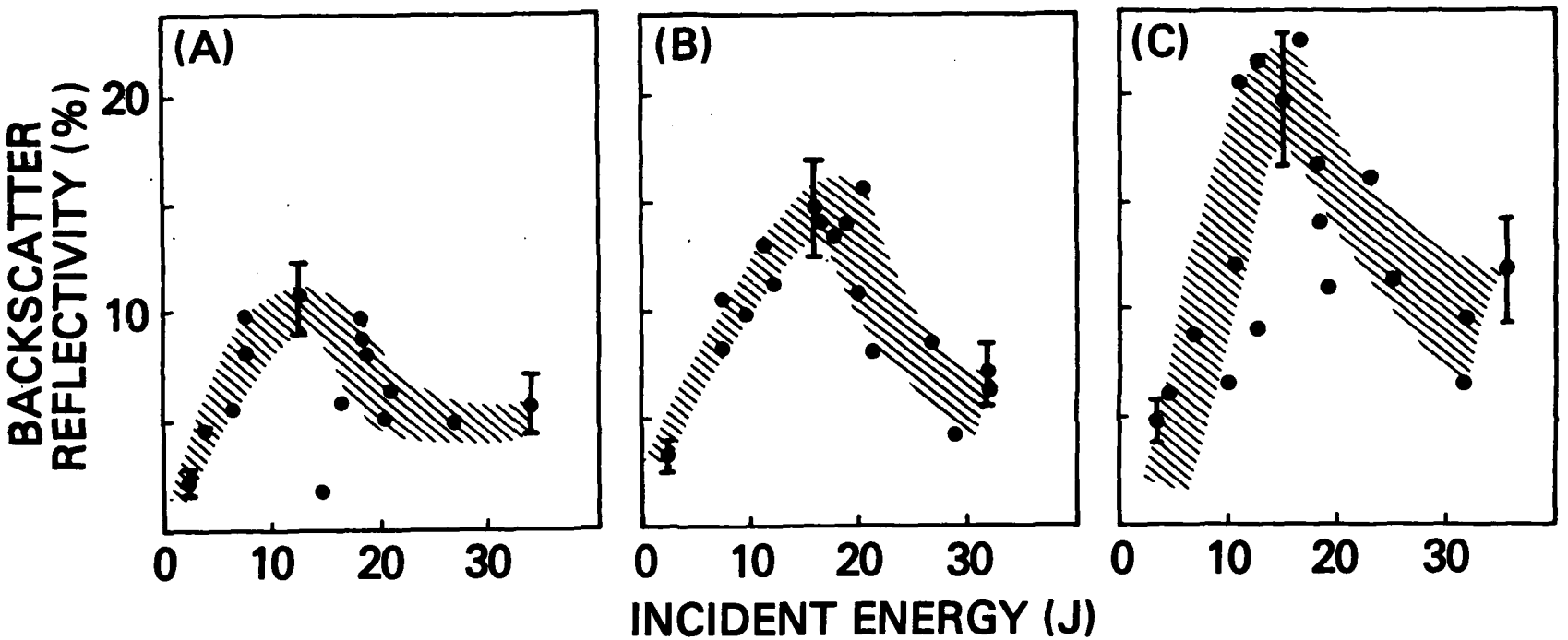

Fig. 2. Backscatter reflectivities for: (A) short, (B) medium, and (C) long-scalelength background plasmas.

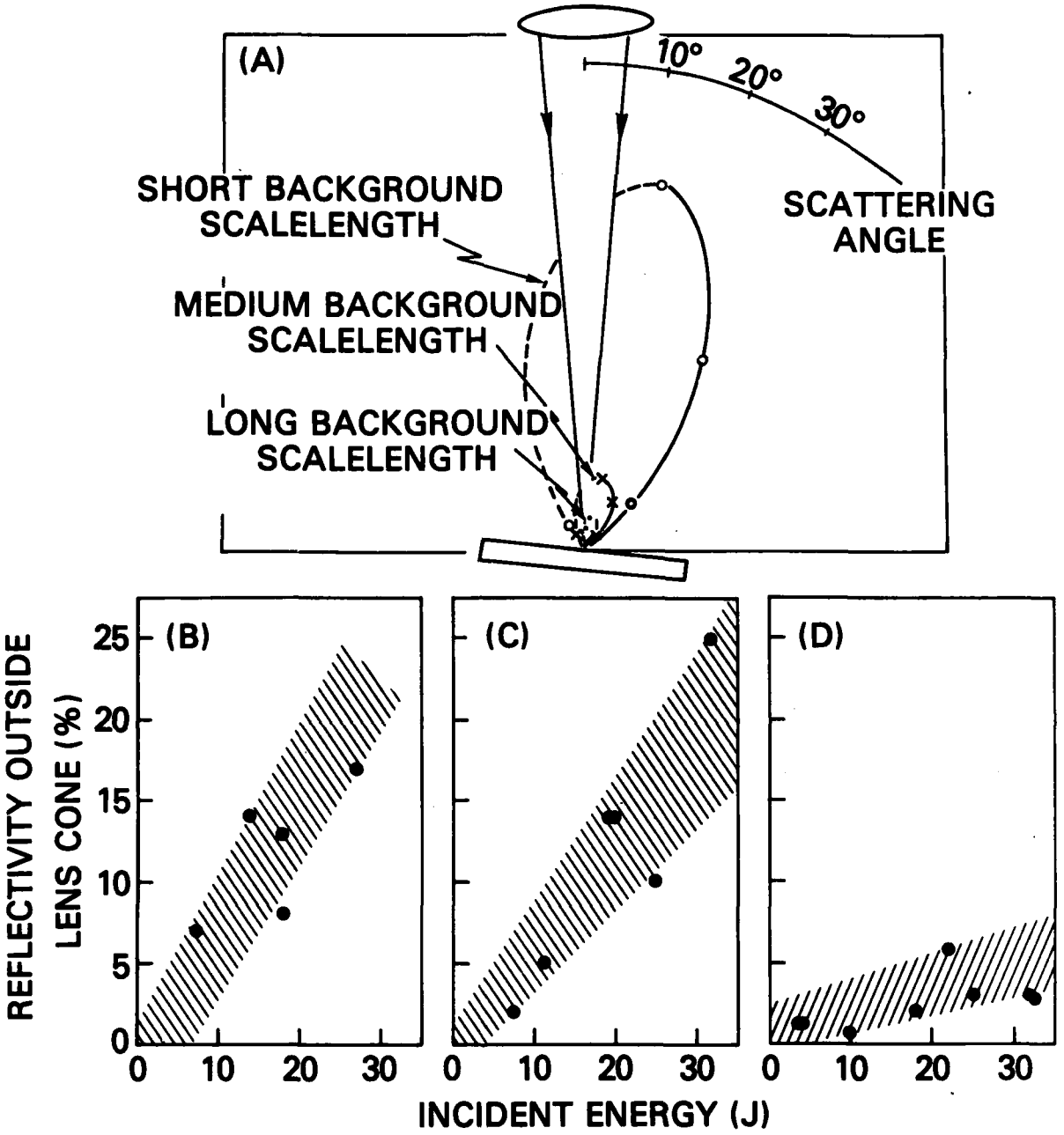

Fig. 3. (A) Angular distributions of light scattered outside the lens cone for E ≈ 10 J. Reflectivities, integrated over angles for: (B) short, (C), medium, and (D) long-scalelength background plasmas.

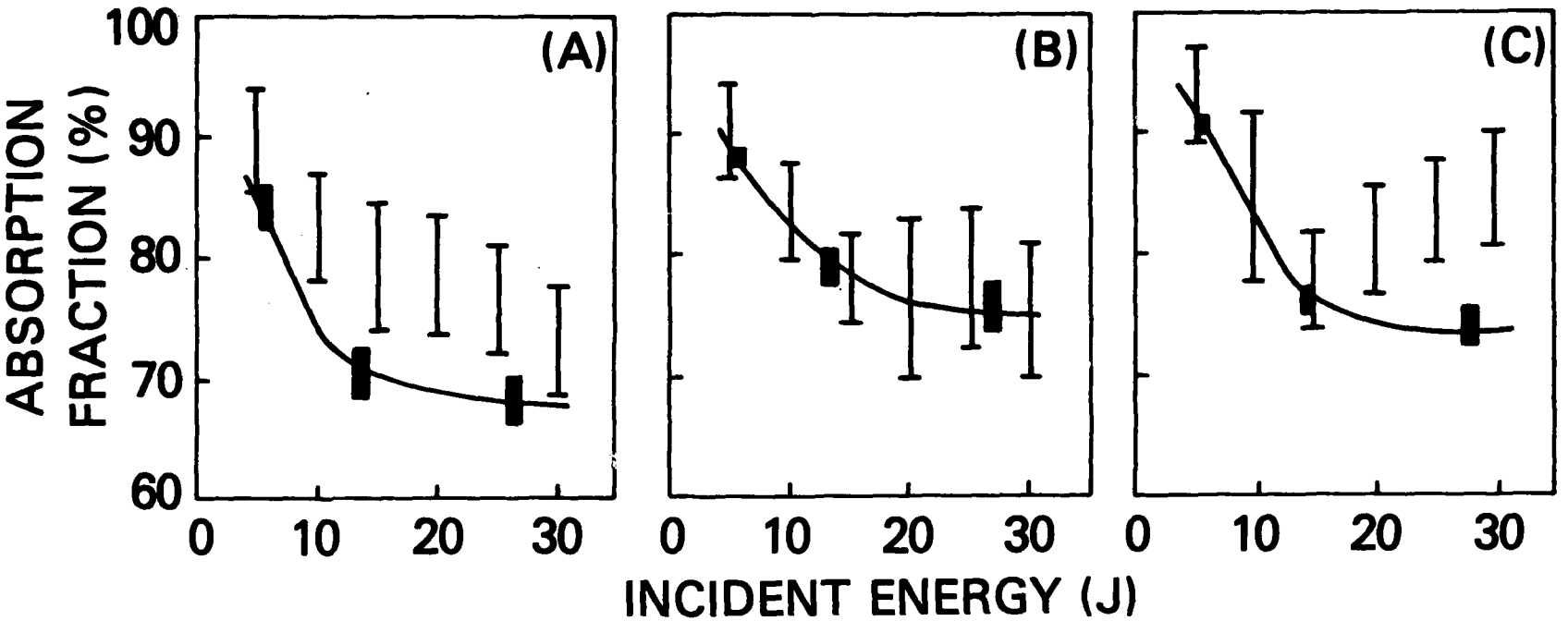

Fig. 4. Comparison between experimental absorption fractions (narrow bars) and calculated collisional absorption (solid curve with wide bars to indicate uncertainties) for (A) short, (B) medium, and (C) long-scalelength background plasmas.

REFERENCES

1. V.L. Ginzburg, The Propagation of Electromagnetic Waves in Plasmas, (Pergamon Press, Oxford, 1970).

2. K. Estabrook and W.L. Kruer, Phys. Rev. Lett. 40, 42 (1978) and references contained therein.

3. T.W. Johnston and J.M. Dawson, Phys. Fluids 16, 722 (1973).

4. C.S. Liu, in Advances in Plasma Physics, v. 6, eds. A. Simon and W.B. Thompson (Wiley, New York, 1976), pp. 121 ff, and references contained therein.

5. J. Gardner, et al., NRL Memorandum Report No. 5170 (1983, to be published).

6. F.C. Young, et al., NRL Memorandum Report No. 5174 (1983, unpublished).

7. J.A. Stamper, et al., NRL Memorandum Report No. 5173 (1983, unpublished).

8. S.E. Bodner, J. Fus. Energy 1, 221 (1981) and references contained therein.

END

FILMED

12-83

DTIC